Electron Transfer Driven by Proton Fluctuations in a Hydrogen-Bonded Donor−Acceptor Assembly†

Justin M. Hodgkiss, Niels H. Damrauer, Steve Pressé, Joel Rosenthal, and Daniel G. Nocera*

Department of Chemistry, 6-335, Massachusetts Institute of Technology, 77 Massachusetts Avenue, Cambridge, Massachusetts 02139-4307

Received: November 19, 2005; In Final Form: May 12, 2006

The temperature-isotope dependence of proton-coupled electron transfer (PCET) for a noncovalent molecular dyad is reported. The system consists of an excited-state Zn(II) porphyrin that transfers an electron to a naphthalene diimide acceptor through an amidinium-carboxylate interface. Two different isotope effects are observed for variant temperature regimes. A reverse isotope effect (i.e., $k_H/k_D < 1$) is observed as T approaches 120 K ($k_H/k_D = 0.9$, 120 K), whereas a normal isotope effect (i.e., $k_H/k_D > 1$) is recovered as the temperature is increased ($k_H/k_D = 1.2$, 300 K). The transition between these limits is smooth, with a crossover temperature of $T \sim 160$ K. These observations are in accordance with charge-transfer dynamics that are susceptible to bath-induced fluctuations in the proton coordinate.

Introduction

When electron transfer (ET) is coupled to proton motion, in what is termed proton-coupled electron transfer (PCET),[1,2] the electron and proton influence each other thermodynamically and kinetically. The driving force, reorganization energy and the electronic coupling depend parametrically on the coordinate of the coupled proton.[3−6] Experimental[7−9] and theoretical[3−6,10,11] investigations designed to explore how this coupling manifests itself in systems that undergo formal proton transfer in concert with electron transfer conclude, not surprisingly, that X−H bond breaking motion is a critical degree of freedom in the transition state for ET. The proton coordinate is additionally modulated by vibrations and bath-induced fluctuations not involved in X−H bond breaking. To date, no measurements or theories have been able to assess directly the microscopic nature of proton-coupling in PCET reactions in which the proton is incompletely transferred. Such reactions are especially important in biology since ET in many proteins and enzymes is supported along pathways exhibiting hydrogen bond contacts between amino acid residues and polypeptide chains.[12,13] Of the various H-bond contacts in biology, guanidinium-carboxylate salt-bridges derived from arginine-aspartane interactions (Scheme 1) are common owing to their role as stabilizing structural elements.[14,15] They are found in natural systems which include RNA stem loops,[16] zinc finger/DNA complexes,[17,18] and the active sites of dihydrofolate reductase,[19] cytochrome *c* oxidase,[20,21] and siroheme sulfite reductase (SiRHP).[22] While the overall structure of a guanidinium-carboxylate interface is ideal for supporting proton transport along an ET pathway, the interface muddles PCET investigations because guanidinium presents multiple binding modes to carboxylate as shown in Scheme 1; kinetics measurements of donor−acceptor pairs bridged by guanidinium-carboxylate can be complicated by multiple equilibria. The complexity arising due to several binding modes may be circumvented by employing an amidinium-carboxylate salt-bridge. This retains the two N−H bonds of the guanidinium-carboxylate salt-bridge while preserving only one specific binding mode for carboxylate. We have exploited this salt-bridge to examine PCET reactions for which the electron and proton-transfer coordinates are collinear.[23−26] The model system (**1-H:2**) shown in Scheme 2 is comprised of a Zn(II) porphyrin photoreductant (**1-H**) and a naphthalene diimide electron acceptor (**2**) assembled via an amidinium-carboxylate salt-bridge where the amidinium is attached to the porphyrin and the carboxylate is attached to the naphthalene diimide.[27,28] In this system, the PCET reaction may be followed by monitoring the growth and decay of the porphyrin cation radical transient absorption (k_{PCET}(fwd) = 9

SCHEME 1

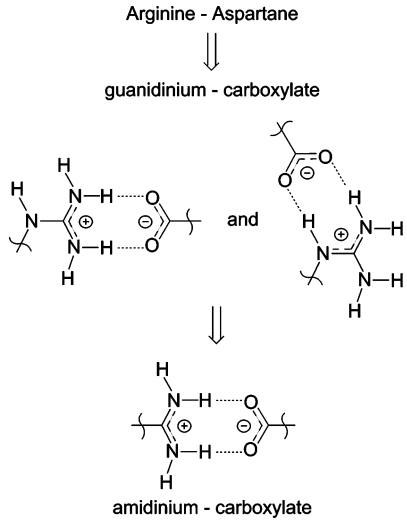

SCHEME 2

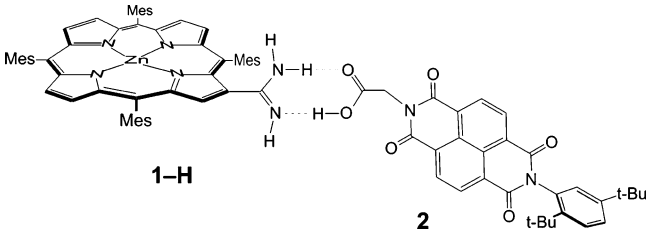

† Part of the special issue "Robert J. Silbey Festschrift".

* Corresponding author.

10.1021/jp056703q CCC: $33.50
Published on Web 06/27/2006

$\times 10^8$ s^{-1} and k_{PCET}(rev) $= 14 \times 10^8$ s^{-1}).[29] The forward rate constant is attenuated by nearly 2 orders of magnitude when compared with ET measured for a dyad consisting of nearly identical donor and acceptor moieties positioned in a comparable geometry, but via covalent bonds rather than H-bonds.[30] Since the thermodynamic driving force and solvent reorganization energies for ET in these two systems are comparable, the large reduction in rate implies that H-bonds in our model system attenuate the electronic coupling between the electron donor and acceptor. This observation suggests that the two-point H-bond is a bottleneck for electronic coupling between the donor and acceptor. Thus, this system may be ideal for elucidating PCET mechanisms in systems not involve X−H bond breaking, i.e., nonradical PCET pathways.

In general, deuterium isotope effects (k_H/k_D) measured for PCET reactions will depend on the sensitivity of the electronic coupling to the proton's position. Accordingly, we set out to interrogate the microscopic role of the intervening protons in our system by measuring the isotope effect on the PCET rate constant as a function of temperature. In our studies k_H refers to the rate of ET observed through a protonated interface (**1-H:2**) while k_D is the corresponding rate through a deuterated interface (**1-D:2**.) We show that these experiments allow us to begin unraveling the role of proton fluctuations in governing PCET reactions through biologically relevant H-bond interfaces.

Experimental Section

Materials. 2-Methyltetrahydrofuran (2-MeTHF), (Spectroscopic grade, Aldrich) was dried using standard methods and stored under vacuum. Individual ampules of D_2O (Cambridge Isotope Laboratories) were used for isotopic exchange experiments. **1-H** was converted to **1-D** by rapid mixing with D_2O. The reaction is facile because the four amidinium protons are the only kinetically labile protons on the porphyrin. Previously reported procedures were used for the preparation and characterization of porphyrin **1-H**,[31] naphthalene diimide **2**,[27] and Zn(II) tetramesitylyporphyrin (ZnTMP).[31]

Physical Methods. Samples for variable temperature transient emission experiments were prepared according to the following procedure: An aliquot (10^{-7} mol) of dry porphyrin **1-H** was dissolved in a minimal volume of THF and added to a 1.0-mL borosilicate short-stem glass ampule (Kimble-Kontes), which was attached to a high-vacuum adaptor. The neck of the ampule had previously been stretched in a flame to facilitate easy sealing in the final stage of sample preparation. In the quenching experiments, 4 equiv of dry naphthalene diimide **2** were also added, and 4 equiv of benzoate were added in the case of the benzoate control experiments. For the experiments requiring deuterium isotope exchange, a few drops of D_2O were added to the solution before closing the ampule to the atmosphere, shaking and leaving for about 15 min. Following this time the transferring solvent and D_2O was removed under vacuum, and the sample was heated on a high vacuum manifold for at least 2 h to remove any residual water. 1.0 mL of dry 2-MeTHF was added to the ampule by vacuum transfer. Under the pressure ($<10^{-6}$ Torr) of the high vacuum manifold, the ampule was then flame-sealed with the solution frozen during the sealing process. These high-vacuum manipulations ensured that that samples remained isolated from the environment and free of water, which otherwise disrupts H-bonding between the donor and acceptor.

Variable temperature experiments employed a modular cryogenic refrigeration system (Air Products and Chemicals). The system consists of a single stage helium compressor (model 1RO2A) connected via hoses to an expander module (model DE-202) with a heating element and temperature controller (Scientific Instruments, 9600-5). The instrument is interfaced with a custom-made computer program in order to automate the temperature sequencing. The expander module is fitted with a laboratory interface (model DMX-1) that consists of a vacuum shroud and glass windows for fluorescence spectroscopy in a right-angled configuration. The chamber is continuously pumped to maintain a vacuum ($\sim 10^{-4}$ Torr) and the sample is mounted on a copper block inside. The thermocouple was calibrated with three temperatures achieved by immersing the sample-holder in liquid nitrogen (77 K), an ice bath (273 K), and leaving it at ambient laboratory temperature (293 K).

The excitation source for the transient emission experiments was a chirped-pulse amplified Ti:sapphire laser system that has been described elsewhere.[27] In this experiment the 100-fs, 800-nm output of the regenerative amplifier was frequency-upconverted in a visible optical parametric amplifier (BMI Alpha-1000) to produce 560-nm excitation pulses for resonant excitation of the Q-band of porphyrin **1**. In this experiment, the excitation was vertically polarized and attenuated to between 50 and 250 nJ/pulse.

Transient emission kinetics were measured using a Hamamatsu C4334 Streak Scope streak camera that has also been described elsewhere.[32] The emission spectrum (from 580 to 720 nm) was collected at the magic angle ($\theta_m = 54.7°$) relative to the vertical polarization of the excitation source. A 10-ns or a 20-ns timebase was used.

The temperature controller and streak camera were computer controlled and synchronized so that the entire temperature range (120−300 K) could be sampled in an automated fashion. In a typical experiment, the sample was left to equilibrate in the dark to a given temperature set-point for 17 min. This was followed by 13 min of fluorescence data collection before moving to the next temperature set-point (typically 10 K away) where equilibration followed by fluorescence measurement was repeated. Different temperature sequences and larger temperature increments (30 K) were also used with longer equilibration times ($\sim$23 min). The data were found to be independent of the sequence employed, confirming that ample time was given for sample temperature equilibration prior to data collection. In the cases where an experiment was started in the low temperature range it was left for approximately 2 h to ensure that it had reached the temperature set-point.

T-dependent lifetimes of **1-H(D)**, and **1-H(D):benzoate** were measured over the 120−300 K temperature range 3−4 times (each with freshly made samples). The emission lifetimes for these compounds were extracted from the streak camera data by integrating 15-nm and 40-nm slices of the emission peaks centered at 612 and 665 nm, respectively, and fitting to a monoexponential decay function. *T*-dependent lifetimes of **1-H(D):2** were measured over the same temperature range 5 times (each with freshly made samples). These data were analyzed in the same way as described above, except that they were fit to a biexponential decay functions, with the longer lifetime component fixed to the time-constant measured for **1-H(D)** for each temperature. Lifetimes from repeated experiments were averaged in all cases.

Results

PCET occurs from the S_1 excited state of **1-H** in the **1-H:2** assemblies. Accordingly, characterization of the *T*-dependence of the spectral properties of the S_1 state was warranted prior to undertaking *T*-dependent PCET measurements. 2-MeTHF was chosen for our studies for several reasons. First, tetrahydrofurans

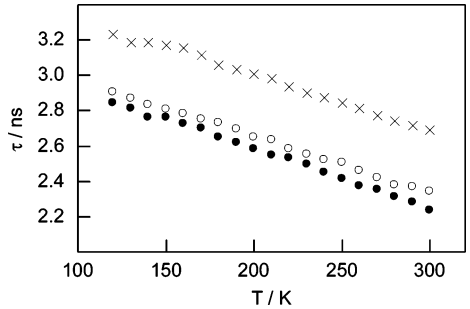

Figure 1. *T*-dependence of the fluorescence lifetimes of **1-H** (solid circles), **1-D** (open circles), and ZnTMP (crosses) in the solvent 2-MeTHF.

do not disrupt amidinium-carboxylate two point bonds and thus support the formation of PCET assemblies.[27] Second, they axially bind the Zn(II) porphyrin which prevents the formation of aggregates characterized by amidine-zinc linkages between different molecules of **1**.[27,33] Finally, 2-MeTHF remains optically transparent at low *T*. The S_1 excited states of the porphyrins were generated by resonant excitation of the $Q_{1,0}$ absorption band of **1** using 560-nm laser pulse excitation. The maxima of $Q_{0,0}$ and $Q_{1,0}$ fluorescence bands at 612 and 660 nm, respectively, are slightly red-shifted from the same bands of ZnTMP ($\lambda_{em,max} = 595$ and 645 nm), which does not bear the amidinium functionality. Porphyrin **1** and ZnTMP exhibited minimal fluorescence spectral shifts over 120−300 K.

Figure 1 shows the *T*-dependent fluorescence lifetimes of porphyrin **1-H**, **1-D**, and ZnTMP in the absence of quencher. We limited our measurements to *T*'s above 120 K to ensure that dynamics associated with the glass-to-solvent transition ($T_g = 86$ K) or rate-limiting solvent dynamics were not complicating our observed kinetics. The fluorescence lifetimes inherent to Zn porphyrins (without introducing additional quenching processes such as electron or energy transfer) are dominated by radiative rates plus nonradiative rates of intersystem crossing (k_{ISC}) to form the triplet excited states. Typically the T_1 state is formed with a quantum yield in excess of 0.9.[34,35] As seen in Figure 1, the three systems show the same functional dependence of lifetime versus *T*, consistent with previous *T*-dependence studies of Zn porphyrins in 2-MeTHF.[36] This indicates that the ISC process itself is thermally activated. The fluorescence lifetimes of **1-H** and **1-D** are significantly shorter than the reference molecule, ZnTMP. This result reflects electronic perturbations to the porphyrin macrocycle in **1-H** and **1-D** by the amidinium functionality, as indicated by the small shifts in the energies of the absorption and emission maxima for these compounds relative to ZnTMP. In addition, the fluorescence lifetime for the **1-D** is always longer than that of **1-H**, corresponding to a modest but statistically significant isotope effect of ~1.03 (τ_{obs}(**1-D**)/τ_{obs}(**1-H**)) throughout the *T*-range studied. The observed isotope effect is ascribed to the coupling of nuclear degrees of freedom involving the amidinium protons to the S_1 excited state of the Zn porphyrin chromophore. That the **1-H** and **1-D** lifetimes are shorter than ZnTMP suggests that coupling of the amidinium functionality to the porhyrin system accelerates the intersystem crossing process in **1**.

Figure 2 shows the *T*-dependent fluorescent lifetimes of **1-H:benzoate** and **1-D:benzoate**, respectively, in 2-MeTHF. Because the benzoate is not capable of quenching the S_1 excited state via the typical mechanisms of ET, PT, or energy transfer, these experiments probe the ISC dynamics for systems exhibiting an H-bonded amidinium. Accordingly, these systems provide an excellent reference rate (k_0) for S_1 deactivation in the absence of actual PCET. For both protonated and deuterated analogues,

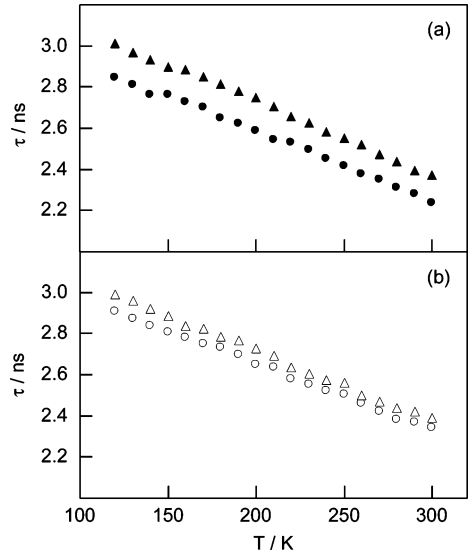

Figure 2. (a) *T*-dependence of the fluorescence lifetimes of **1-H** (solid circles), compared with **1-H:benzoate** (solid triangles) in the solvent 2-MeTHF. (b) *T*-dependence of the fluorescence lifetimes of **1-D** (open circles), compared with **1-D:benzoate** (open triangles) in the solvent 2-MeTHF.

the lifetimes are found to *increase* upon addition of benzoate. This is consistent with our previous work at room temperature.[27] The lifetime increase is ascribed to the restricted motion of the amidinium protons when they participate in a H-bonding interaction. This reduces their contributions to nonradiative deactivation pathways of the S_1 excited state. Unlike cases where PCET is involved (vide infra), the difference between the S_1 excited-state lifetimes for bound and unbound forms is modest. Thus, it is difficult to resolve an isotope effect (τ_{obs}(**1-D:benzoate**)/τ_{obs}(**1-H:benzoate**)) with reasonable fidelity.[37] There are several other noteworthy points regarding the **1-H(D):benzoate** lifetime measurements. The slopes of the curves in Figures 1 and 2 are the same, indicating that formation of the salt-bridge does not perturb the activation barrier for ISC. Also, we do not observe any significant spectral shift for absorption or emission following association with the benzoate. This attests to the weak electronic coupling between the porphyrin chromophore and the amidinium functionality due to rotation of the amidinium group out of plane with respect to the conjugated π-system of the porphyrin macrocycle. Steric clashing between the external hydrogens of the amidinium group and the mesityl group at the adjacent *meso* position of the porphyrin ring cause the amidinium to cant by ~76°.[27]

The above results establish the underlying *T*-dependent behavior of the S_1 excited state of **1-H(D)**, against which the PCET kinetics of the associated salt-bridge assemblies, **1-H(D):2**, may be compared. Transient absorption spectroscopy has demonstrated that PCET accounts for the quenching of the S_1 excited state of **1-H** upon association with **2**.[27] With PCET established, we preferred to study the *T*-dependence of PCET by time-resolved emission because fluorescence is much easier to detect, and PCET rates can be measured with reduced experimental error. NMR spectroscopy shows that the amidinium-carboxylate salt-bridge is established by a two-point interaction and that π-stacking between the donor and acceptor does not occur.[27] At room *T*, the association constant for the formation of **1-H:2** ($K_{assoc} \sim 2.4 \times 10^4$ M^{-1}, THF, 298 K)[27] corresponds to approximately 85% bound and 15% unbound at the concentrations employed in these experiments. The presence of two species in equilibrium results in a biexponential

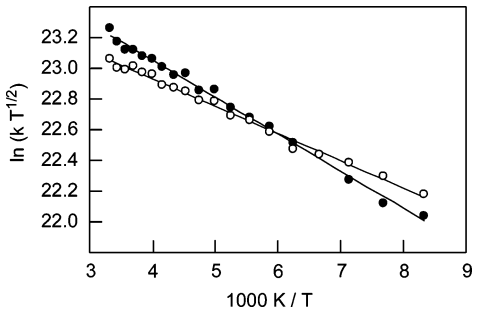

Figure 3. *T*-dependence of the rate of PCET in **1-H:2** (solid circles) and **1-D:2**(open circles) in the solvent 2-MeTHF. Data are presented in a modified Arrhenius form with linear fits.

fluorescence decay because the lifetime of **1-H(D):2** is significantly shorter that that of **1-H(D)** over the entire *T*-range studied. As previously noted,[27] the ratio of short:long lifetime components is related to the association constant. The observed ratio of short:long lifetime components at room temperature in these experiments corresponds to that expected from the known association constant, reassuring us that water has been successfully excluded during sample preparation. As expected, the ratio of short:long lifetime components increases as *T* is decreased, reflecting the *T*-dependence of the association constant. To reduce the number of variables for data analysis, the longer decay component was fixed to the lifetime measured for the free porphyrin, **1-H(D)** at each value of *T*. The extracted shorter lifetime (at each value of *T*) corresponds to association pairs, **1-H(D):2** where PCET is occurring. We note that since the loss of the S_1 state in **1-H(D):2** is time-resolved, PCET rates can be obtained with a high degree of accuracy despite variation in the absolute fluorescence intensity as well as the ratio of the two lifetime components. With S_1 lifetimes in hand, the rate of PCET at each *T* may be determined from the difference between the reciprocal lifetimes of **1-H(D)** bound to benzoate and **2** (i.e., $k_{PCET} = k_{obs} - k_0 = 1/\tau_{(\mathbf{1-H(D):2})} - 1/\tau_{(\mathbf{1-H(D):benzoate})}$). In this treatment, the quenching rate is compared against the lifetime of the **1-H(D):benzoate** complex as opposed to the lifetime of unbound **1-H(D)** in order to account for the perturbation of the S_1 lifetime due to H-bond formation.

Figure 3 presents the *T*-dependent ET rates for **1-H(D):2** in the form of a modified Arrhenius plot ($\ln(k_{PCET}\cdot T^{1/2})$ vs $1/T$). That k_H is not equal to k_D over most of the *T*-range studied is consistent with the contention that the ET rate is sensitive to the position and/or motion of the intervening protons of the salt-bridge. Surprisingly, the ratio k_H/k_D also varies over the *T*-range examined. In the high-*T* limit, the rate of PCET in **1-H:2** is faster than in **1-D:2** ($k_H/k_D \sim 1.2$ (300 K)). With decreasing *T*, the rate of PCET for **1-H:2** drops more rapidly than that for **1-D:2**. This leads to the unusual situation of a deuterium kinetic isotope effect that diminishes and inverts with decreasing *T*. ET through **1-H:2** is actually slower than for **1-D:2** at low *T* ($k_H/k_D \sim 0.9$ (120 K)). Both protonated and deuterated datasets show a linear dependence of $\ln(k_{PCET}\cdot T^{1/2})$ vs $1/T$.

Discussion

The data presented in Figure 3 may be initially analyzed with the semiclassical Marcus equation,[38,39]

$$k_{ET} = \sqrt{\frac{\pi}{\hbar^2 \lambda k_B T}}|V|^2 \exp\left[-\frac{(\Delta G^0 + \lambda)^2}{4\lambda k_B T}\right] \qquad (1)$$

The slope of the linear fits reveals the activation energy of the PCET reactions. Since the driving force $\Delta G°$ is known ($\Delta G° = -0.58$ eV),[40] the nuclear reorganization energy λ can be determined. The thermodynamic parameters for these PCET reactions are provided in Table 1. The calculated activation energies of $2.08 \pm 0.08 \times 10^{-2}$ eV and $1.54 \pm 0.07 \times 10^{-2}$ eV for **1-H:2** and **1-D:2**, respectively, are small when compared to the overall thermodynamic driving force of the reaction. The reorganization energies of $\lambda_H = 0.85 \pm 0.01$ eV and $\lambda_D = 0.80 \pm 0.01$ eV are relatively close to a ballpark estimate that combines a Marcus outer-sphere reorganization energy of ~0.7 eV[41] and ~0.2−0.3 eV for the inner-sphere contribution.[42,43] Using $\Delta G°$ and λ_H (or λ_D), the electronic coupling term *V* may be determined from the y-intercept of the plot per eq 1. The values of $V_H = 2.4 \pm 0.1$ cm^{-1} and $V_D = 1.9 \pm 0.1$ cm^{-1} for **1-H:2** and **1-D:2**, respectively, are small when compared to the coupling constants ($V \sim$ 10's of cm^{-1}s) measured for covalently linked systems that place similar electron donors and acceptors in a comparable geometry as **1-H:2**.[30,36,44,45] The ~100-fold attenuation in the rate of **1-H:2** compared with the previously published covalently bonded analogue[30] is largely attributed to the bottleneck of electronic coupling associated with the H-bonded interface.

TABLE 1. Thermodynamic and Kinetic Parameters Measured for 1-H:2 and 1-D:2

assembly	$\Delta G°$/eV	E_{act}(obs)[a]/ eV	λ_{obs}[a]/eV	$\lvert V\rvert$[a]/cm^{-1}
1-H:2	−0.56	$2.08 \pm 0.08 \times 10^{-2}$	0.85 ± 0.01	2.4 ± 0.1
1-D:2	−0.56	$1.54 \pm 0.07 \times 10^{-2}$	0.80 ± 0.01	1.9 ± 0.1

[a] Obtained from fitting to eq 1, assuming $\Delta G°$ is *T*-independent.

Despite predicting the general magnitude of fitted parameters, semiclassical Marcus treatments of ET rates cannot account for the observed k_H/k_D crossover. Admittedly, our calculations of solvent reorganization energy and Coulombic corrections to the driving force neglected the *T*-dependence of the solvent dielectric constant, even though the dielectric constant and refractive index of 2-MeTHF are known to increase with decreasing *T*.[46] Reconsideration of this simplifying assumption allows perturbations of the barrier height with decreasing *T*,[47,48] which in turn, could cause deviation from linearity in the Arrhenius plots of both **1-H:2** and **1-D:2**. However, it cannot account for a difference between the two isotopic forms. Other explanations of anomalous *T*-dependences in ET reactions are dynamic solvent parameters such as viscosity and longitudinal relaxation time,[45,49,50] as well as conformational changes within donor−acceptor systems that occur with changes in *T*.[44,51] Likewise, these effects do not discriminate between the isotopic forms of the bridge and consequently do not account for the observed k_H/k_D crossover in the *T*-dependence measurements of the PCET reactions of **1-H:2** versus **1-D:2**.

PCET theories step beyond conventional ET theories in their explicit treatment of PT.[52−54] Formulations of PCET obtain rate expressions that resemble a Marcus treatment of ET (eq 1) with the following notable exceptions: (i) the transferring proton (or deuteron) contributes to the determination of λ and $\Delta G°$, and (ii) the rate is obtained from a weighted sum over all possible proton (deuteron) donor vibrational states and a sum over Franck−Condon overlaps involving each possible combination of proton (deuteron) donor and acceptor vibrational states. In most cases, the sum in (ii) is over high-frequency two-atom vibrations of the transferring proton (deuteron).

The PCET problem is simplified by considering a proton (deuteron) tunneling from its ground vibrational donor state to one of its vibrational acceptor states. In this case *V*, in addition to λ and $\Delta G°$, includes contributions from the transferring proton (deuteron). Strictly speaking, the entirety of the isotopic depend-

ence of these PCET models is recovered in their *T*-independent *V*, which now includes a Franck−Condon overlap term for the transferring proton (deuteron). The resulting k_H/k_D is thus *T*-independent in this limit. Hammes-Schiffer and co-workers have attributed the system-specific nature of the isotopic dependence in *V* to factors including proton (deuteron) donor−acceptor distance, endothermicity of the reaction, and solvent polarity.[55] On the other hand, a *T*-dependence in k_H/k_D emerges if the total rate expression is written as a sum over many independent rates, e.g., rates originating from multiple channels available for PCET as a function of increasing *T* through, for example, excited vibrational state contribution. It is unclear, however, why this would lead to crossover in k_H/k_D with changing *T*.

Features of a new model of vibrationally assisted PCET (involving no proton transfer) by Pressé and Silbey are described in order to provide a simple explanation for the *T*-dependence of k_H/k_D.[56] Briefly, in this model the electron tunneling barrier is made susceptible to fluctuations in a vibrational mode localized to the H-bonding bridge linking the electron donor and acceptor. These fluctuations result in a shift in the proton (deuteron) coordinate. We emphasize the importance of the electronic coupling term, because in **1-H:2**, the H-bond is the bottleneck for electronic coupling. A physical model that explains this PCET reaction without transferring a proton is depicted in Figure 4. The electronic coupling term (and consequently the PCET rate) is maximized when a fluctuation displaces the proton coordinate to a position not too far from its equilibrium coordinate, which we label Q_M. The isotope effect observed is then related to the ratio of proton and deuteron probability density at Q_M. Note that for simplicity, Q_M is modeled as a discrete position and it is always a fraction of an Angstrom even in the large Q_M limit. It would be physically reasonable to introduce some dispersion to this function, though it is not necessary to account for the *T*-dependence of k_H/k_D. The model leads to the following rate expression:

$$k \propto \sqrt{\frac{\pi}{\hbar^2 \lambda k_B T}}|V'|^2 \exp\left[-\frac{(\Delta G^\circ + \lambda)^2}{4\lambda k_B T}\right]\left(1 + O\left(\exp\left[-\frac{\hbar\omega}{2k_B T}\right]\right)\right) \quad (2a)$$

In this expression, $O(\exp[-\hbar\omega/2k_BT])$ denotes all higher order terms which become important as $\exp(-\hbar\omega/2k_BT) \sim 1$, ω is a low-frequency vibration localized to the H-bond involving mostly motion of the proton (deuteron), and *V*' is the renormalized electronic coupling constant

$$|V'| = \frac{|V|}{\sqrt{A}} \exp\left[-\frac{{Q_M}^2}{A}\right] \quad (2b)$$

where *A* is a quantum factor obtained through thermal averaging and it is larger for the proton than the deuteron.

At very low *T* when none of the vibrational states in the H-bond are excited, only the lowest order term in the model survives and k_H/k_D is either normal or reversed, based on the magnitude of Q_M. For large Q_M, i.e., when the proton coordinate must deviate substantially from its equilibrium position to maximize the electronic coupling term, the isotope effect is normal because the quantum factor, *A*, is larger for the proton. This result is reasonable because the proton wave function is more diffuse and better samples the region near Q_M. The opposite holds true for small Q_M at low *T* where the deuteron wave function better samples the region.

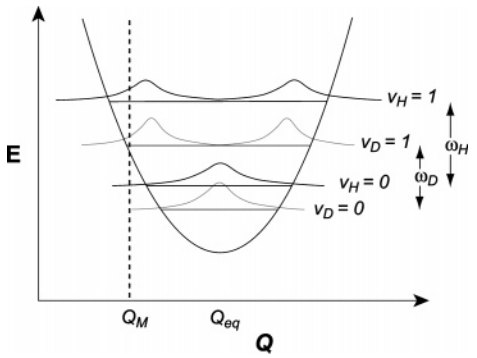

Figure 4. Depiction of the essential features of the model proposed to account for the observed *T*-dependence of the isotope effect. The ET rate is related to the vibrational wave function probability density at the point Q_M (dashed line), where electronic coupling is maximized. *Q* is the coordinate in the vibrational mode that has particular significance in promoting ET. The ω of this mode is low enough that thermally populated vibrational excited states can contribute to overlap at Q_M. In addition, ω is decreased upon deuteration, leading to differentiation between ET rates mediated by protons (black probability densities) and deuterons (gray probability densities), depending on the magnitudes of Q_M, ω, and k_BT.

The behavior in the high-*T* regime is also simple to understand. Provided the frequency of the mode in the bridge undergoing the relevant fluctuations is not too high, we can think of several excited vibrational states of this mode contributing to the dynamics of ET. If enough states are populated, the resulting thermally weighted displacement in the proton coordinate leads to a larger electronic coupling for large Q_M, and the resulting isotope effect is normal. The opposite holds for small Q_M.

Given the model for intermediate *T* (which applies to the lowest *T*'s in our experimental data), with large Q_M it is possible to find a *T* where the thermally induced shift in the deuteron probability density for a deuterated interface begins contributing to the PCET rate. However, in the case of the protonated interface, such contributions to the PCET rate are relevant only at higher *T*'s owing to the higher frequency of proton vibrations. This means that one can obtain a reverse isotope effect, even for large Q_M, in the intermediate-*T* regime by considering vibrations that undergo a change in frequency upon deuteration. The normal isotope effect is recovered with increasing *T* as the lowest lying excited states of the H-bond vibration of interest begin contributing to the PCET rate. Of course, this contribution is amplified if the vibrational frequency of the mode involving the proton (deuteron), undergoing the relevant fluctuations, is low enough that thermally populated vibrational states comprise an important contribution to the PCET rate. Finally, we now see that empirical fits of PCET data with Marcus theory should invoke an effective *T*-dependence in the electronic coupling, as the H-bonded interface makes this term susceptible to fluctuations.

Concluding Remarks

Protons that mediate electronic coupling between an electron donor and acceptor, but do not transfer, result in an attenuation of the rate of ET. This type of PCET reaction is important for charge transport through proteins and enzymes since the tertiary structure is often established by extensive H-bond networks. Collinear PCET assemblies of the type described here, **1-H(D):2**, allow this biologically important PCET reaction to be probed by analysis of the *T*-dependence of k_H/k_D. Microscopic insight is gained when well-defined model systems are subjected to direct spectroscopic rate measurements, rather than indirect

probes of, for example, enzyme turnover numbers, or reaction yields. We find that a signature of this type of PCET reaction is a dependence of the ratio k_H/k_D on T, which leads to a crossover in this case. The crossover manifests itself when (1) the H-bonding bridge is the bottleneck for electronic coupling; (2) the mediating protons must deviate from their equilibrium positions in order to optimize electronic coupling for ET; (3) the coordinate of the proton is susceptible to T-dependent fluctuations; and (4) the activation energy inherent to the ET process[57,58] is low enough that thermally activated proton dynamics are not obscured. The model suggests that low-frequency vibrations in the H-bond bridging the electron donor and acceptor account for the unusual crossover T-dependence of k_H/k_D. Future experiments will employ transient IR and 2D−IR methods to probe directly the nuclear degrees of freedom directly of PCET reactions.

Acknowledgment. We thank R. J. Silbey for helpful discussion, Dr. Chen-Yu Yeh for synthesis of **1**, and we are grateful to Peter Galvin for assistance with computer hardware. N.H.D. gratefully acknowledges the NIH for support of a postdoctoral fellowship. S.P. acknowledges a fellowship from the NSERC. This work was supported a grant from the National Institutes of Health (GM 47274).

References and Notes

(1) Turró, C.; Chang, C. K.; Leroi, G. E.; Cukier, R. I.; Nocera, D. G. *J. Am. Chem. Soc*. **1992**, *114*, 4013−4015.

(2) Chang, C. J.; Chang, M. C. Y.; Damrauer, N. H.; Nocera, D. G. *Biochim. Biophys. Acta* **2004**, *1655*, 13−28.

(3) Cukier, R. I.; Nocera, D. G. *Annu. Rev. Phys. Chem*. **1998**, *49*, 337−369.

(4) Cukier, R. I. *J. Phys. Chem*. **1994**, *98*, 2377−2381.

(5) Hammes-Schiffer, S. In *Electron Transfer in Chemistry;* V. Balzani, Ed.; Wiley-VCH: Weinheim, Germany, 2001; Vol. 1.1.5; pp 189−214.

(6) Hammes-Schiffer, S. *Acc. Chem. Res*. **2001**, *34*, 273−281.

(7) Biczók, L.; Gupta, N.; Linschitz, H. *J. Am. Chem. Soc*. **1997**, *119*, 12601−12609.

(8) Sjödin, M.; Styring, S.; Åkermark, B.; Sun, L.; Hammarström, L. *J. Am. Chem. Soc*. **2000**, *122*, 3932−3936.

(9) Roth, J. P.; Lovel, S.; Mayer, J. M. *J. Am. Chem. Soc*. **2000**, *122*, 5486−5498.

(10) Iordanova, N.; Decornez, H.; Hammes-Schiffer, S. *J. Am. Chem. Soc*. **2001**, *123*, 3723−3733.

(11) Carra, C.; Iordanova, N.; Hammes-Schiffer, S. *J. Am. Chem. Soc*. **2003**, *125*, 10429−10436.

(12) Beratan, D. N.; Onuchic, J. N.; Hopfield, J. J. *J. Chem. Phys*. **1987**, *86*, 4488−4498.

(13) Beratan, D. N.; Onuchic, J. N.; Winkler, J. R.; Gray, H. B. *Science* **1992**, *258*, 1740−1741.

(14) Kumar, S.; Nussinov, R. *ChemBioChem* **2002**, *3*, 604−617.

(15) Bosshard, H. R.; Marti, D. N.; Jelesarov, I. *J. Mol. Recognit*. **2004**, *17*, 1−16.

(16) Puglisi, J. D.; Chen, L.; Frankel A. D.; Williamson, J. R. *Proc. Natl. Acad. Sci. U.S.A.* **1993**, *90*, 3680−3684.

(17) Pavletich, N. P.; Pabo, C. O. *Science* **1991**, *252*, 809−817.

(18) Berg, J. M. *Acc. Chem. Res.* **1995**, *28*, 14−19.

(19) Howell, E. H.; Villafranca, J. E.; Warren, M. S.; Oatley, S. J.; Kraut, J. *Science* **1986**, *231*, 1123−1128.

(20) Ramirez, B. E.; Malmström, B. G.; Winkler, J. R.; Gray, H. B. *Proc. Natl. Acad. Sci. U.S.A.* **1995**, *92*, 11949−11951.

(21) Brzezinski, P. *Biochemistry* **1996**, *35*, 5611−5615.

(22) Crane, B. R.; Siegel, L. M.; Getzoff, E. D. *Science* **1995**, *270*, 59−67.

(23) Roberts, J. A.; Kirby, J. P.; Nocera, D. G. *J. Am. Chem. Soc*. **1995**, *117*, 8051−8052.

(24) Kirby, J. P.; Roberts, J. A.; Nocera, D. G. *J. Am. Chem. Soc*. **1997**, *119*, 9320−9326.

(25) Roberts, J. A.; Kirby, J. P.; Wall, S. T.; Nocera, D. G. *Inorg. Chim. Acta* **1997**, *263*, 395−405.

(26) Chang, C. J.; Brown, J. D. K.; Chang, M. C. Y.; Baker, E. A.; Nocera, D. G. In *Electron Transfer in Chemistry;* Balzani, V., Ed.; Wiley-VCH: Weinheim, Germany, 2001; Vol. 3.2.4, pp 409−461.

(27) Damrauer, N. H.; Hodgkiss, J. M.; Rosenthal, J.; Nocera, D. G. *J. Phys. Chem. B* **2004**, *108*, 6315−6321.

(28) The Zn(II) porphyrin amidinium was prepared as a chloride salt, and the naphthalene diimide carboxylate was prepared as a tetramethylamonium salt.

(29) The reverse PCET reaction is not actually the microscopic reverse of the forward reaction. The forward reaction is initiated by the S_1 excited state of the Zn porphyrin. Yet the reverse reaction ultimately recovers the porphyrin ground state, possibly via intermediates involving triplet excited states of the Zn porphyrin or the naphthalene diimide.

(30) Osuka, A.; Yoneshima, R.; Shiratori, H.; Okada, S.; Taniguchi, S.; Mataga, N. *Chem Commun*. **1998**, 1567−1568.

(31) Yeh, C.-Y.; Miller, S. E.; Carpenter, S. D.; Nocera, D. G. *Inorg. Chem*. **2001**, *40*, 3643−3646.

(32) Loh, Z.-H.; Miller, S. E.; Chang, C. J.; Carpenter, S. D.; Nocera, D. G. *J. Phys. Chem. A* **2002**, *106*, 11700−11708.

(33) Otsuki, J.; Iwasaki, K.; Nakano, Y.; Itou, M.; Araki, Y.; Ito, O. *Chem. Eur. J*. **2004**, *10*, 3461−3466.

(34) Gradyushko, A. T.; Tsvirko, M. P. *Opt. Spectrosc*. **1971**, *31*, 291−295.

(35) Rodriguez, J.; Kirmaier, C.; Holten, D. *J. Am. Chem. Soc.* **1989**, *111*, 6500−6506.

(36) Winters, M. U.; Pettersson, K.; Mårtensson, J.; Albinsson, B. *Chem. Eur. J*. **2005**, *11*, 562−573.

(37) In the benzoate experiments, both bound and unbound porphyrins are expected to exist in reasonable concentrations at the spectroscopic concentrations employed. Yet the apparent similarity between bound and unbound lifetimes means that the **1-H(D):benzoate** data cannot be reliably fit to a biexponential decay function, despite there being a good physical basis for doing so. Consequently, the empirically fit monoexponential decay functions are biased to some extent by the fraction of unbound porphyrin that also contributes to the signal, and this fraction is subject to experimental error.

(38) Marcus, R. A.; Sutin, N. *Biochim. Biophys. Acta* **1985**, *811*, 265−322.

(39) Marcus, R. A. *J. Chem. Phys.* **1956**, *24*, 966−978.

(40) The published driving force for this system ($\Delta G° = -0.46$ eV, ref 27) neglected the solvent-dependent Coulombic term ($\Delta G(\epsilon)$). Using the Born equation, we estimate an additional 0.12 eV towards the driving force for ET in this system in 2-MeTHF, based on a donor−acceptor distance of 13 Å, and radii of 5 and 4 Å for the donor and acceptor, respectively. Additionally, a small T-dependence in the Coulombic term should arise due to the T-dependence of the solvent dielectric constant, however we neglected this minor effect in the fitting of reorganization energies. This issue is addressed at another point in the text.

(41) Calculated using the Marcus dielectric continuum model for 2-MeTHF, based on a donor−acceptor distance of 13 Å, and radii of 5 and 4 Å for the donor and acceptor, respectively.

(42) Archer, M. D.; Gadzekpo, V. P. Y.; Bolton, J. R.; Schmidt, J. A.; Weedon, A. C. *J. Chem. Soc., Faraday Trans. 2* **1986**, *82*, 2305−2313.

(43) Gaines, G. L., III; O'Neil, M. P.; Svec, W. A.; Niemczyk, M. P.; Wasielewski, M. R. *J. Am. Chem. Soc.* **1991**, *113*, 719−721.

(44) Davis, W. B.; Ratner, M. A.; Wasielewski, M. R. *J. Am. Chem. Soc*. **2001**, *123*, 7877−7886.

(45) Harrison, R. J.; Pearce, B.; Beddard, G. S.; Cowan, J. A.; Sanders, J. K. M. *Chem. Phys*. **1987**, *116*, 429−448.

(46) Liu, J.-Y.; Bolton, J. R. *J. Phys. Chem.* **1992**, *96*, 1718−1725.

(47) Khundkar, L. R.; Perry, J. W.; Hanson, J. E.; Dervan, P. B. *J. Am. Chem. Soc.* **1994**, *116*, 9700−9709.

(48) Liang, N.; Miller, J. R.; Closs, G. L. *J. Am. Chem. Soc*. **1989**, *111*, 8740−8741.

(49) Heitele, H.; Michel-Beyerle, M. E.; Finckh, P. *Chem. Phys. Lett*. **1987**, *138*, 237−243.

(50) Rempel, U.; von Maltzan, B.; von Borczyskowski, C. *Z. Phys. Chem*. **1991**, *170*, 107−116.

(51) Leland, B. A.; Joran, A. D.; Felker, P. M.; Hopfield, J. J.; Zewail, A. H.; Dervan, P. B. *J. Phys. Chem.* **1985**, *89*, 5571−5573.

(52) Cukier, R. I. *J. Phys. Chem*. **1995**, *99*, 16101−16115.

(53) Cukier, R. I. *J. Phys. Chem. B* **2002**, *106*, 1746−1757.

(54) Soudackov, A.; Hammes-Schiffer, S. *J. Chem. Phys*. **1999**, *111*, 4672−4687.

(55) Decornez, H.; Hammes-Schiffer, S. *J. Phys. Chem. A* **2000**, *104*, 9370−9384.

(56) Pressé, S.; Silbey, R. *J. Chem. Phys.* **2006**, *124*, 164504−7.

(57) While we have focused on the dynamic variation of electronic coupling through proton motion, the driving force and reorganization energy for ET could potentially dominate the T-dependence of ET. However, in this case, we are able to learn about the nature of the proton-mediated electronic coupling because the magnitude of the driving force and reorganization energy are similar enough that the resulting activation energy is low. This is analogous to studies on the distance-dependence of ET rates in modified proteins. There, electron donors and acceptors are selected to minimize the activation energy for ET, highlighting the variation of the electronic coupling term with donor−acceptor distance (e.g., see ref 58).

(58) Winkler, J. R.; Gray, H. B. *Chem. Rev*. **1992**, *92*, 369−379.